Applied Energy 187 (2017) 326–337

Contents lists available at ScienceDirect

Applied Energy

journal homepage: www.elsevier.com/locate/apenergy

PV array power output maximization under partial shading using new shifted PV array arrangements

N. Belhaouas [a,b,c], M.-S. Ait Cheikh [b], P. Agathoklis [c], M.-R. Oularbi [d], B. Amrouche [a], K. Sedraoui [e], N. Djilali [e,f,*]

[a] Centre de Développement des Energies Renouvelables, CDER, B.P. 62, Route de l'observatoire, Bouzaréah 16340, Alger, Algeria
[b] Laboratoire des dispositifs de communication et de conversion photovoltaïque, École Nationale Polytechnique, BP 182, El Harrach, Alger, Algeria
[c] Department of Electrical and Computer Engineering, University of Victoria, Victoria, BC V8W2Y2, Canada
[d] Davidson Consulting, 37 Rue Marcel Dassault, 92100 Boulogne-Billancourt, France
[e] Renewable Energy Group, King Abdulaziz University, Jeddah, Saudi Arabia
[f] Department of Mechanical Engineering, and Institute for Integrated Energy Systems, University of Victoria, BC V8W 3P6, Canada

HIGHLIGHTS

- New physical PV array arrangements are proposed to mitigate partial shading effects.
- Performance analysis performed under a range of cloud and shading pattern scenarios.
- Shifted PV arrangements power-voltage curves exhibit a single peak.
- Global Maximum Power Point is readily determined.
- Power dissipation is reduced and energy output is optimized.

GRAPHICAL ABSTRACT

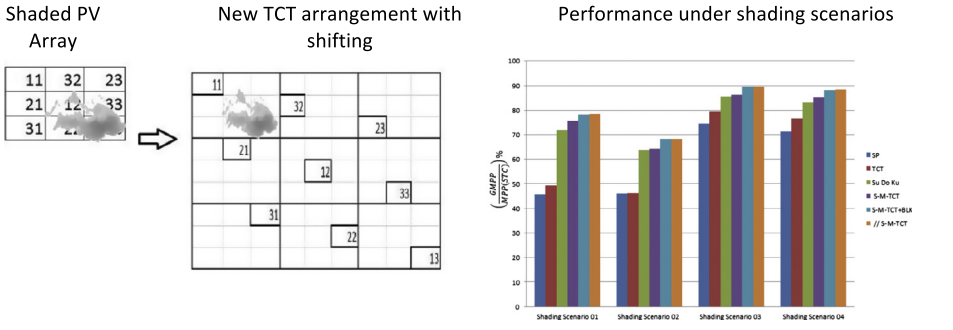

ARTICLE INFO

Article history:
Received 22 August 2016
Received in revised form 29 October 2016
Accepted 11 November 2016

Keywords:
Photovoltaic (PV)
Partial shading effects
Bypass and blocking diodes
PV array configuration
Maximum power point tracking (MPPT)
Solar energy

ABSTRACT

Partial shading can dramatically reduce the power output of a PV array as well as complicate operation by causing multiple peaks to appear in the power-voltage (P-V) characteristic curve. The extent of these problems depends not only on the shading area but also and much more significantly on the shading pattern. In this paper three new physical PV array arrangements are proposed to mitigate partial shading effects. The arrangements are based on maximizing the distance between adjacent PV modules within a PV array by appropriately arranging modules in different rows and columns without changing the electrical connections. A systematic analysis is performed to assess the proposed PV array arrangements under different shading patterns and scenarios, and to compare performance with existing configurations. The new arrangements are shown to effectively (i) redistribute shading patterns over the entire PV array, (ii) minimize protection diodes power dissipation, (iii) eliminate multiple peaks, and (iv) maximize power output. The analysis considers shading scenarios related to cloud shape, size, transmissivity and passage over an array. The new configurations simplify operation and improve performance significantly compared to the reference Series-Parallel (SP) and Total Cross Tied (TCT) configurations: the characteristic P-V curves exhibit a single peak allowing tracking of the maximum power point with a simple controller removing the need for complex controller algorithms and costly hardware, and the power output gains range from 19 to 140% compared to SP, and 13 to 68% compared to TCT.

1. Introduction

Solar power generation is growing fast in many parts of the world [1,2] driven by cost reduction, economic incentives and

* Corresponding author at: Department of Mechanical Engineering, and Institute for Integrated Energy Systems, University of Victoria, BC V8W 3P6, Canada.
E-mail address: ndjilali@uvic.ca (N. Djilali).

http://dx.doi.org/10.1016/j.apenergy.2016.11.038
0306-2619/

the needs for meeting growth in electricity demand while reducing reliance on fossil fuels. However, several challenges need to be addressed to allow its effective deployment [3].

The power output of solar photo voltaic (PV) arrays, the focus of this paper, is optimal only under full irradiation conditions. Under partial shading, solar irradiance and the efficiency of the PV array can decrease dramatically. Shading can be caused not only by clouds, but also by buildings, trees, soiling, dust and even PV cell cracking and ageing [4]. The extent and impact of shading depend on the application and end use, e.g. solar PV power plants, building-integrated photovoltaics, rural electrification or electric vehicles [5,6]. Alleviating the effect of partial shading is an important practical challenge [7].

In addition to reducing the PV array power output, partial shading also causes the power-voltage (P-V) curve to exhibit multiple peaks. This can in turn cause conventional Maximum Power Point Tracking (MPPT) techniques to be trapped at the Local Maximum Power Point (LMPP), which leads to significant power losses. A range of conventional MPPT techniques under partial shading have been devised to address this problem, and their classification, key features and main limitations are reviewed in [8,9]. Notable recent contributions include fuzzy-logic controllers [10], neural-network based methods [11] and sophisticated genetic algorithms to reach the Global Maximum Power Point (GMPP) [12]. Some of the key issues that remain are the complexity and cost of these algorithms, and the need for embedded sensors in some cases [13].

Strategies to mitigate shading effects are based on the observation that shading pattern rather than shaded area is the primary factor determining PV output power losses [14]. A number of researchers have consequently attempted to address the problem using electrical configurations based on interleaving of PV modules [15], and a new research avenue was opened by recent studies showing that partial shading losses can be reduced by modifying the electrical configuration of a P-V array [16,17].

The Series-Parallel (SP) configuration is commonly used in the PV industry, but other PV configurations to mitigate shading effect losses have been reported and include: Bridge Linked (BL), Honey Comb (HC) and Total Cross Tied (TCT) [18]. Although comparative studies have shown the TCT configuration gives the best results in terms of PV Power output for almost all types of shading [19], several researchers still focus their work on partial shading mitigation to the SP configuration [20].

Another configuration modification is the Electrical Array Reconfiguration (EAR) which consists of dynamically changing the electrical connections of PV modules. The main idea in the EAR strategy is to adapt the PV using a controllable switching matrix to select a configuration that reduces as much as possible the partial shading loss for a given shading pattern. This strategy requires a fully reconfigurable array and necessitates sensors and switches that increase system complexity and cost [21–24].

Static reconfiguration is an alternative to EAR that achieves a balance between cost, complexity and efficiency. This approach relies on finding a PV module arrangement with a fixed predefined TCT configuration [25]. The predefined reconfiguration is designed such that the shading effect is minimized for a variety of shading patterns. For example, in [26] a Su Do Ku puzzle pattern is shown to effectively mitigate partial shading and maximize power generation. The Su Do Ku pattern is however only applicable to 9×9 PV modules, and furthermore requires consideration of the impact of protection diodes, especially blocking diodes. PV modules arrangements for arbitrary PV array sizes have been proposed to overcome this limitation [27]. Such arrangements and others discussed in [14,15,25] operate with an array having an equal number of rows and columns, and are restricted to modifying the electrical connections of PV modules which are in the same physical PV array row. As a consequence, shading dispersion is limited and protection diodes power consumption is high. Similar approaches to change the PV module arrangement within a PV array under TCT and other configurations are discussed for example in [28–30]. These arrangements still locate PV modules in the same column and are in fact almost identical to Su Do Ku. In addition, these arrangements have not taken into account the power dissipation of blocking and bypass diodes and, in most cases, have only been applied to small PV arrays.

The brief review highlights the need for improved strategies to deal with the multiple maxima exhibited by the P-V curves, since on the one hand algorithms that avoid trapping at the Local Maximum Power Point (LMPP) and succeed in finding the Global Maximum Power Point (GMPP) are complex and expensive, and on the other hand PV module reconfigurations proposed to date are limited and suffer from various degrees of power dissipation. Here, we present a new reconfiguration strategy that effectively distributes PV modules under shading over the entire PV array. This is achieved with an electrical connection pattern between PV modules that are far apart but not on the same row and/or column. The proposed PV array arrangement leads to P-V characteristic curves that eliminate the LMPPs and exhibit only one easily identifiable peak corresponding to the GMPP. This makes it easier to track the maximum power point with no need for complex MPPT controllers or the added expense of embedded sensors. To further increase the efficiency of the proposed arrangement we also introduce bypass and blocking diodes in each PV module instead of the commonly used blocking diode at the top of a PV array string. This helps reshape the P-V characteristic and effectively ensures one peak even under severe partial shading conditions.

The paper proceeds with a brief overview of the mathematical model of PV arrays and the simulation and analysis of the impact of protection diodes in PV arrays under shading conditions, followed by a description of the new PV array arrangement and a comparative analysis of its performance under a variety of partial shading scenarios.

2. System description

2.1. PV model

A large number of models have been developed to characterize PV modules under varying atmospheric conditions [31]. These models are non linear and rely on a variety of techniques for parameter identification [32,33].

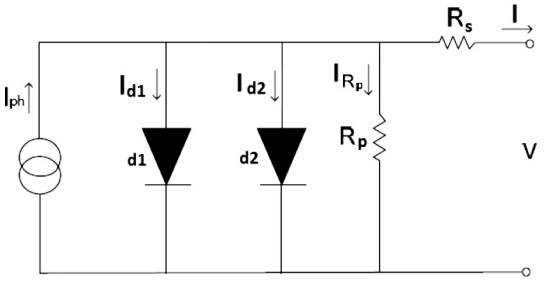

Fig. 1. Equivalent two-diode circuit model of a PV cell.

Table 1
Parameters of MSX-60 PV module.

I_{sc}	3.8 A	K_v	−80 mV/°C
V_{oc}	21.1 V	K_i	3 m%/°C
I_{mpp}	3.5 A	N_{cell}	36
V_{mpp}	17.1 V	P_{max}	58 W

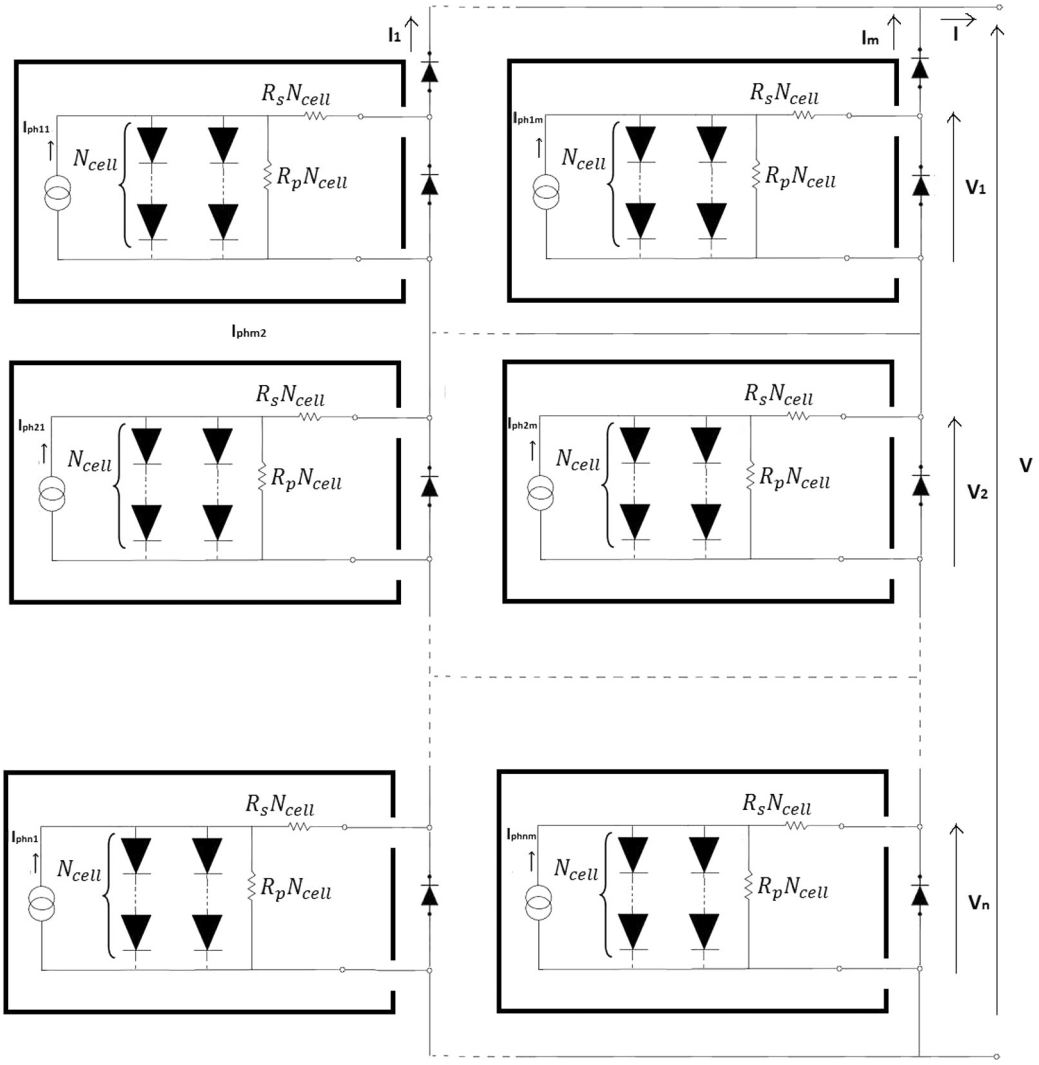

Fig. 2. Block diagram of the PV array consisting of M columns and N rows with bypass and blocking diodes.

In this study the analysis is based on the two-diode model (see Fig. 1) which has been widely used, especially for partial shading effects, and provides higher accuracy than the one diode model [34,35]. The current I generated by the PV module is expressed as a function of the generation current I_{Ph}, which depends on the irradiation, the temperature resistors (R_s, R_p), and the number of PV cells (N_{cell}) connected in series.[1] Mathematically, this is expressed by Eqs. (1)–(3), these equations are derived from the electrical circuit shown in Fig. 1 and are described in greater detail in [36,37].

$$I = I_{Ph} - I_{d1} - I_{d2} - \frac{V + IR_S N_{cell}}{R_p N_{cell}} \quad (1)$$

$$I_{Ph} = (I_{Ph(STC)} + K_i(T - T_{(STC)}))\frac{G}{G_{(STC)}} \quad (2)$$

$$I_{d,i=1,2} = I_{0i} \exp\left(\frac{V + IR_S N_{cell}}{A_i\left(\frac{KT}{q}\right)N_{cell}}\right) \quad (3)$$

with the variables and parameters represent:

STC: standard test conditions.
$I_{Ph(STC)}$: photo current at STC [A].
$T_{(STC)}$: PV cell temperature at STC [K].
T: PV cell temperature [K].

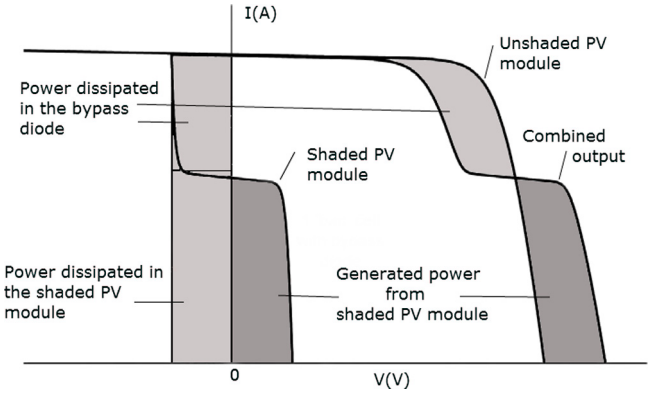

Fig. 3. Impact of bypass diode on the (I-V) PV characteristic of two PV modules connected in series.

[1] Here, the PV cells are connected in series to build up a PV module.

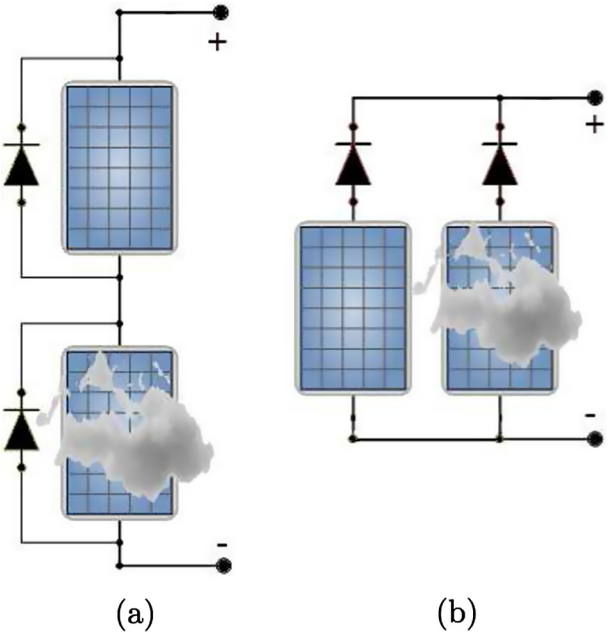

Fig. 4. Two PV modules (one of which is shaded) connected in (a) series with bypass diodes protection, (b) parallel with blocking diodes protection.

$G_{(STC)}$: irradiance at STC [W/m^2].
G: solar irradiance in [W/m^2].
K_i: temperature short circuit coefficient.
I_0: the reverse saturation current [A].
q: electron charge (1.602×10^{-19} C).
k: Boltzmann constant (1.38×10^{-23} J/K).
A_i: diode ideality constants.
R_s: series resistance [Ω].
R_p: parallel resistance [Ω].
N_{cell}: number of series cells.
I_{0i}: reverse saturation current.
A_i: diode ideality factor of diode 1 and 2 respectively.

The parameters required in the above equations are generally available from manufacturers data-sheets. The parameters in this study correspond to the MSX-60 PV module and are given in Table 1.

2.2. Matlab/Simulink simulations

The two-diode PV module model was implemented using multi Matlab/Simulink subsystems and building on different submodels and Simulink toolboxes [16,36]. The connection between PV modules can be made by simple branch connections at different connection points as shown in Fig. 2. Similarly, the blocking and bypass diodes can be connected in series or in parallel with the PV modules [38]. The number of PV modules in series and parallel determine the PV array size and consequently the PV array power output. Iph_{ij}, I_j and V_i is the photo current, current and voltage of the PV array row and column position (i,j).

2.3. Minimizing the impact of partial shading

Shading affects directly the PV module/array performance and output power [39]. Since it is usually not possible to avoid partial shading due to clouds, dirt, etc. [40], it is important to investigate the most favorable relationship between shading pattern type, interconnection, configuration and PV module arrangement in order to increase PV array power yield and eliminate multiple peaks in the P-V characteristic [16,26]. Use of an optimal interconnection such as TCT configuration or the TCT with PV module arrangement appears to be particularly suitable for minimizing shading effects on the PV array [41]. Furthermore, power losses as well as multi peaks and PV degradation can also be reduced by adding bypass and blocking diode [42,43]. The equations of the PV module/array remain unchanged, since the electrical connections of TCT or TCT with PV module arrangement remain the same.

2.4. Impact of bypass and blocking diodes under partial shading

In principle, all PV modules within a PV array have the same characteristics. However the PV array power output is limited by

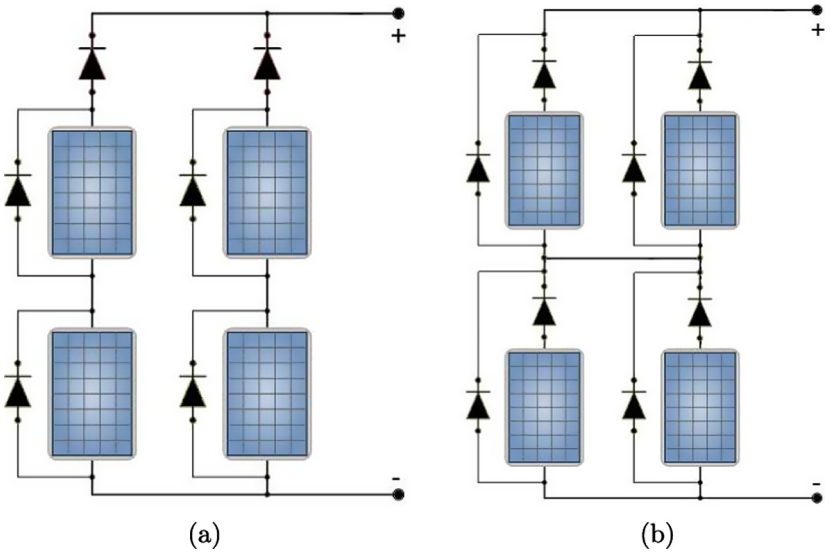

Fig. 5. 2 × 2 PV array with bypass diodes across each PV module, and blocking diodes (a) in the top of each PV string within PV array connected in SP configuration, (b) across each PV module within PV array connected in TCT configuration.

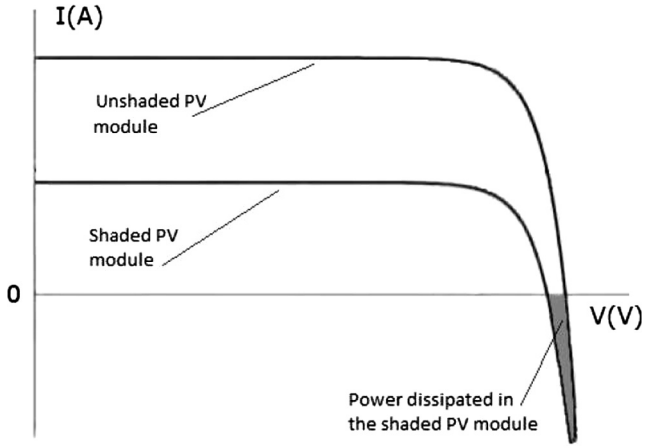

Fig. 6. Impact of blocking diode on the (I-V) PV characteristic of two PV modules connected in parallel.

the shaded modules that dissipate significant part of the generated power. The energy dissipated leads to overheating and hence damage and degradation of the shaded PV modules [44]. One solution is to add bypass diodes in reverse across each PV module.

Under uniform irradiance, each bypass diode is reverse biased when the PV module is generating power. However, under partial shading conditions the PV module tends to be reverse biased by other PV modules causing bypass conduction [42]. Thus, the bypass diodes will short-circuit the shaded PV module allowing the current to flow through them, thereby reducing the power loss through the shaded PV modules.

Typical power dissipation of the PV array with bypass protection is illustrated in Fig. 3, showing a simulation of a PV string corresponding to the shaded and unshaded PV modules in Fig. 4(a). The combined I-V curves, Fig. 3, obtained by summing individual PV modules I-V curves, include the voltage drop across the bypass diodes when conducting current. Fig. 3 also illustrates the power dissipated in the bypass diode and the shaded PV module. The dissipation power drawn in light gray in Fig. 3 depends on the severity of the shading, diode current conduction, and number of shaded cells per bypass diode. Since power dissipation increases with increasing current through a bypass diode, it is effective to minimize this current by minimizing the PV module number in a string under TCT configuration. The reduced power dissipation in the shaded PV modules is also beneficial in reducing the number of cells per bypass diode or the number of PV modules per string.

Hot spot problems may arise in other ways, e.g. when strings or PV modules are wired in parallel and one of them is shaded. Instead of generating power, such a module would dissipate the power generated by other unshaded modules [45]. This problem can be solved by adding blocking diodes on the top of each string in SP configuration or on each PV module in TCT configuration Fig. 5, thus preventing the reverse current flow through shaded PV modules. Fig. 6 shows the I-V characteristic curve of two PV modules connected in parallel one of which is partially shaded as in Fig. 4(b). The importance of inserting a blocking diode in each PV module within a PV array connected in TCT configuration (Fig. 5(b)) is illustrated in figure (Fig. 6).

3. New PV array arrangement

The connected in TCT with shifting array arrangement presented here is devised to distribute the shadow pattern over the entire PV array and mitigate its impact, and to increase the array energy yield. This arrangement relies on changing the physical location of the PV modules for each PV array in such a way as to

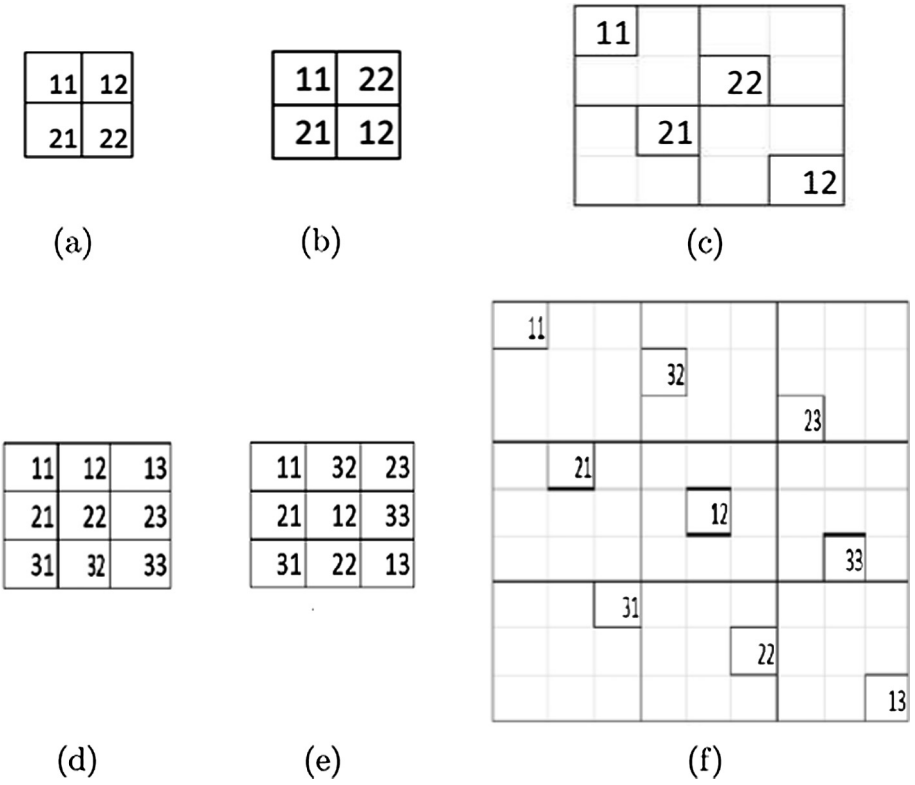

Fig. 7. 2 × 2 PV array: (a) TCT; (b) modified TCT arrangement; (c) modified TCT with shifting; 3 × 3 PV array: (d) TC; (e) modified TCT arrangement; (f) modified TCT with shifting.

improve on the TCT configuration arrangement shown in Fig. 7(a) and (d).

Fig. 7(b) and (e) shows how the changes are implemented in each of the columns of the modified TCT (M-TCT) PV array arrangement. These changes can maximize GMPP and minimize variations between P-V characteristic curve peaks as will be demonstrated is the nest Section. Since the initial electrical connections between PV modules are unchanged, the same model equations apply.

Shifting is introduced to the modified TCT (M-TCT) to decrease the correlation between shaded PV modules and shadow patterns. The idea is to create an empty array ($4 \times 4/9 \times 9$) divided in equal sub-arrays ($2 \times 2/3 \times 3$), and then distribute the PV modules in such way that they are no longer in the same row and column as shown in Fig. 7(c) and (f). The main benefit of the arrangement with shifting is the maximized spatial gap between adjacent PV modules in different columns and rows.

A shortcoming of the M-TCT arrangement with shifting is wasted space as shown in Fig. 7(c) and (f). To address this problem, the extra space is filled up with PV modules from separate PV sub-arrays (from A to I) as shown in Fig. 8(b); the nine PV sub-arrays

11[A]	32[B]	23[C]	22[G]	13[H]	31[I]	33[D]	21[E]	12[F]
21[D]	12[E]	33[F]	32[A]	23[B]	11 [C]	13[G]	31[H]	22[I]
31[G]	22[H]	13[I]	12[D]	33[E]	21[F]	23[A]	11[B]	32[C]
33[C]	21[A]	12[B]	11[I]	32[G]	23[H]	22[F]	13[D]	31[E]
13[F]	31[D]	22[E]	21[C]	12[A]	33[B]	32[I]	23[G]	11[H]
23[I]	11[G]	32[H]	31[F]	22[D]	13[E]	12[C]	33[A]	21[B]
22[B]	13[C]	31[A]	33[H]	21[I]	12[G]	11[E]	32[F]	23[D]
32[E]	23[F]	11[D]	13[B]	31 [C]	22[A]	21[H]	12[I]	33[G]
12[H]	33[I]	21[G]	23[E]	11[F]	32[D]	31[B]	22[C]	13[A]

(a)

11[A]	32[A]	23[A]	11[H]	32[H]	23[H]	32[F]	23[F]	11[F]
21[A]	12[A]	33[A]	21[H]	12[H]	33[H]	12[F]	33[F]	21[F]
31[A]	22[A]	13[A]	31[H]	22[H]	13[H]	22[F]	13[F]	31[F]
23[D]	11[D]	32[D]	32[B]	23[B]	11[B]	23[I]	11[I]	32[I]
33[D]	21[D]	12[D]	12[B]	33[B]	21[B]	33[I]	21[I]	12[I]
13[D]	31[D]	22[D]	22[B]	13[B]	31[B]	13[I]	31[I]	22[I]
32[G]	23[G]	11[G]	23[E]	11[E]	32[E]	11[C]	32[C]	23[C]
12[G]	33[G]	21[G]	33[E]	21[E]	12[E]	21[C]	12[C]	33[C]
22[G]	13[G]	31[G]	13[E]	31[E]	22[E]	31[C]	22[C]	13[C]

(b)

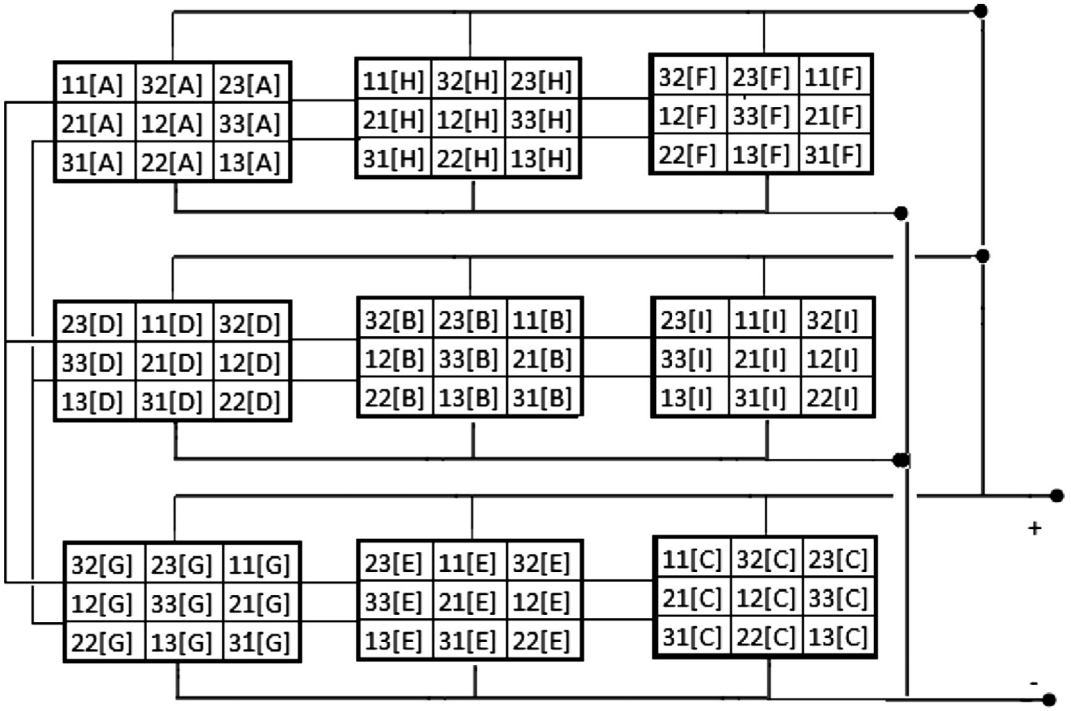

(c)

Fig. 8. (a) Physical location of S-M-TCT arrangement. (b) Electrical connection of S-M-TCT arrangement. (c) Electrical connection of parallel S-M-TCT arrangement.

are arranged by changing their column, row, and even their position, in such a way that each shifted PV sub-array contains only one PV module of each PV sub-array A to I. This is illustrated with the highlighted PV modules of sub array [A] which are distributed all around the 9 × 9 array in Fig. 8(a)); all other PV sub arrays are shifted in the same manner.

The electrical connections of the new shift modified TCT (S-M-TCT) arrangement are shown in Fig. 8(b). In addition to minimizing the correlation between shading patterns and the mismatch losses in the PV array, the efficiency of the new arrangement is also enhanced by inserting blocking diode for each PV module in the S-M-TCT arrangement in contrast to other arrangements and configurations that do not use blocking diodes or use a single one at the top of each PV string. Clearly, the blocking diodes should have the smallest possible resistance to minimize power consumption, especially under uniform irradiance.

Fig. 8(c) shows an alternative approach for the new shifted arrangement in which the sub-array of S-M-TCT arrangement is connected in parallel (// S-M-TCT). This can also mitigate the shading effect and reduce the protection diodes power dissipation.

The performance and energy yield improvement of the proposed PV arrangement are evaluated next for a 9 × 9 PV array under different partial shading conditions and compared to other configurations presented in the literature.

4. Performance assessment

Matlab/Simulink simulations were performed to analyze and evaluate the proposed PV array arrangements in terms of the GMPP and the extent to which the number of peaks are minimized in the P-V characteristics curves.

A PV array with two distinct groups is considered. The first group is completely shaded (no irradiation), while the remaining modules are fully irradiated (1000 W/m^2). The groupings vary for each distinct shading type discussed below. The characteristics of the PV module MSX-60 used in the analysis are given in Table 1.

4.1. Effectiveness of PV array shifting in mitigate partial shading effect

Fig. 9 illustrates the impact of a cloud shadow across a 2 × 2 and a 3 × 3 PV array with two PV array configurations: M-TCT and M-TCT with shifting (for the same cloud shading pattern). Table 2 compares the power output performance of these configurations with the SP and TCT ones. Because all modules of the 2 × 2 array are shaded as shown in Fig. 9(a), the array does not produce any power with the SP, TCT and M-TCT configurations. The shaded 3 × 3 PV array GMPP with these configurations attain only around 35% of GMPP at STC. By applying shifting to the TCT modified configuration, the GMPP of a 2 × 2 PV array increases from zero to about 54%, and 100% of GMPP is achieved for the 3 × 3 PV array.

4.2. Analysis and comparison of different arrangements under different partial shading patterns

To further assess the potential benefits of the new S-M-TCT PV array arrangement performance for different shading types and scenarios, a comparative analysis is performed under identical conditions: temperature $T = 35$ °C and irradiation of the unshaded PV modules of G = 1000 W/m^2, with shaded PV modules considered to be fully covered (G = 0 W/m^2). Table S5 in the Supplementary Material presents GMPP values for all simulated PV array configurations (S-M-TCT, //S-M-TCT, S-M-TCT+BLK, S-M-TCT, Su Do Ku, TCT and SP) under different shading patterns. In the discussion below, the P-V curves are plotted on the same graphs for convenience and the corresponding GMPP values are summarized in separate bar graphs.

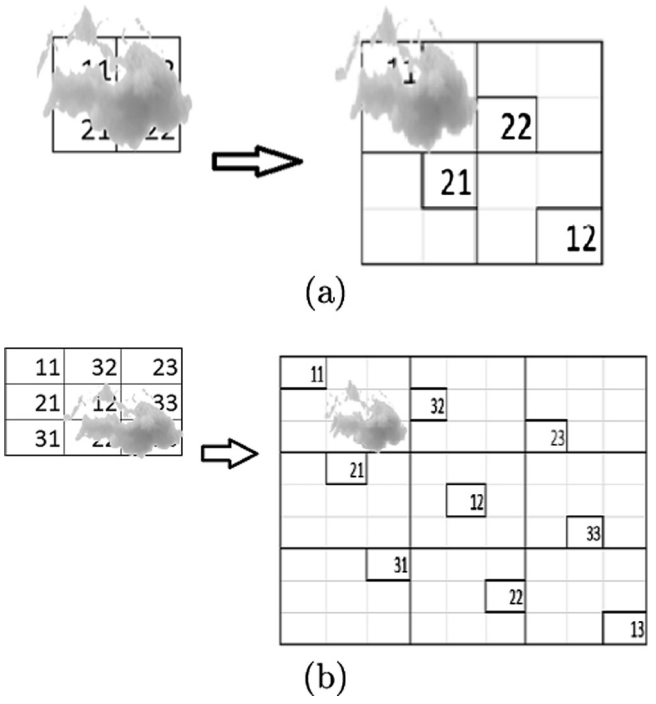

Fig. 9. M-TCT arrangement with and without shifting: (a) 2 × 2 PV array; (b) 3 × 3 PV array.

Table 2
GMPP of various configurations under shading for 2 × 2 and 3 × 3 PV array.

	GMPP with comparison to unshaded PV array			
	2 × 2 PV array		3 × 3 PV array	
	GMPP (W)	GMPP (%)	GMPP (W)	GMPP (%)
SP	0	0	174.60	33.33
TCT	0	0	185.33	35.38
M-TCT	0	0	215.74	41.19
M-TCT with shifting	124.36	54.35	523.80	100

Short and Narrow

The Short and Narrow shading pattern and physical S-M-TCT arrangement is depicted in Fig. 10(a); the electrical connection to disperse the shading pattern for S-M-TCT and //S-M-TCT are shown in Fig. 10(b) and (c) respectively.

All S-M-TCT configurations yield significant power output enhancement and P-V curves with a single peak (MPP) corresponding to the GMPP. This is a result of an array arrangement resulting in identical generated currents for different columns, and even in the same rows in the case of the PV array arrangement with TCT connections. The P-V characteristic curves show that S-M-TCT +BLK, S-M-TCT and the S-M-TCT not only exhibit a single peak but also the highest MPP. Although the Su Do Ku arrangement also yields one peak, its power generation is lower than S-M-TCT. The TCT and SP configurations on the other hand produce multiple peaks (LMPP) and the lowest GMPP. The performance of //S-M-TCT and S-M-TCT+BLK is almost identical, with a slight advantage to the //S-M-TCT (4077 W vs. 4081 W) as shown in Figs. 10(d) and 11. The //S-M-TCT slight advantage is due to the lower energy dissipation associated with fewer blocking diodes and PV modules per PV string. Overall, the power output of the //S-M-TCT and S-M-TCT

11[A]	32[B]	23[C]	22[G]	13[H]	31[I]	33[D]	21[E]	12[F]
21[D]	12[E]	33[F]	32[A]	23[B]	11[C]	13[G]	31[H]	22[I]
31[G]	22[H]	13[I]	12[D]	33[E]	21[F]	23[A]	11[B]	32[C]
33[C]	21[A]	12[B]	11[I]	32[G]	23[H]	22[F]	13[D]	31[E]
13[F]	31[D]	22[E]	21[C]	12[A]	33[B]	32[I]	23[G]	11[H]
23[I]	11[G]	32[H]	31[F]	22[D]	13[E]	12[C]	33[A]	21[B]
22[B]	13[C]	31[A]	33[H]	21[I]	12[G]	11[E]	32[F]	23[D]
32[E]	23[F]	11[D]	13[B]	31 [C]	22[A]	21[H]	12[I]	33[G]
12[H]	33[I]	21[G]	23[E]	11[F]	32[D]	31[B]	22[C]	13[A]

(a)

11[A]	32[A]	23[A]	11[H]	32[H]	23[H]	32[F]	23[F]	11[F]
21[A]	12[A]	33[A]	21[H]	12[H]	33[H]	12[F]	33[F]	21[F]
31[A]	22[A]	13[A]	31[H]	22[H]	13[H]	22[F]	13[F]	31[F]
23[D]	11[D]	32[D]	32[B]	23[B]	11[B]	23[I]	11[I]	32[I]
33[D]	21[D]	12[D]	12[B]	33[B]	21[B]	33[I]	21[I]	12[I]
13[D]	31[D]	22[D]	22[B]	13[B]	31[B]	13[I]	31[I]	22[I]
32[G]	23[G]	11[G]	23[E]	11[E]	32[E]	11[C]	32[C]	23[C]
12[G]	33[G]	21[G]	33[E]	21[E]	12[E]	21[C]	12[C]	33[C]
22[G]	13[G]	31[G]	13[E]	31[E]	22[E]	31[C]	22[C]	13[C]

(b)

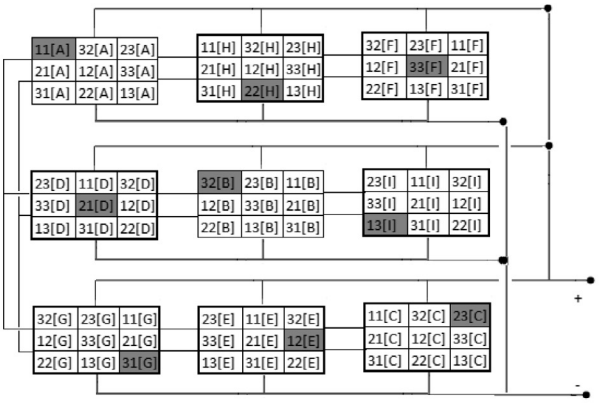

(c)

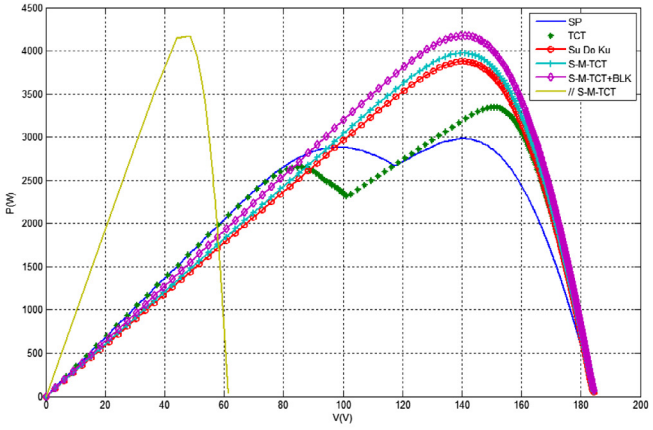

(d)

Fig. 10. Short and Narrow shading pattern: (a) S-M-TCT physical arrangement; (b) S-M-TCT electrical connection; (c) // S-M-TCT electrical connection; (d) P-V characteristics of different PV configuration.

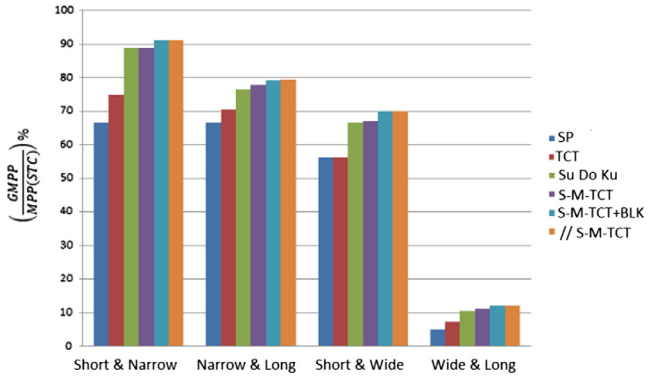

Fig. 11. GMPP (%) for the various configurations and arrangements under different types of shading.

+BLK is 37%, 22%, and 2.7% higher than the SP, TCT and Su Do Ku arrangements respectively.

Narrow and Long

For this shading pattern (Fig. 12), both //S-M-TCT and S-M-TCT +BLK boost the GMPP power output as shown in Fig. 11. The gains are 19% and 12.8% compared to SP and TCT respectively, and 3.2%, 2.1% compared to Su Do Ku and S-M-TCT, with the latter performing slightly better than Su Do Ku. It should be noted again that Su Do Ku and all proposed S-M-TCT arrangements exhibit a single MPP peak, whereas a small LMPP peak is apparent at the beginning of the P-V curve of the other configurations.

Short and Wide

Again the proposed PV array arrangements perform better under the short and wide shading pattern and do not exhibit any LMPP as shown in Fig. 13. The GMPP of //S-M-TCT or S-M-TCT +BLK arrangements are compared to SP, TCT, Su Do Ku, S-M-TCT in Fig. 11 and result in 24.6%, 24.6%, 5.2% and 4.4% power gains respectively.

Wide and Long

In this case the shading pattern (Fig. 14(a)) can be distributed uniformly over an entire PV array by the S-M-TCT arrangement as shown in Fig. 14(b) and (c). The S-M-TCT arrangements still produce the highest GMPP with enhancements of 144% over SP, 68% over TCT and 14% over Su Do Ku as shown in Fig. 11. None of the configurations suffer from LMPPs for this shading pattern.

4.2.1. Partial shading pattern scenarios with different irradiation levels

So far only binary shading was considered for different modules, whereas under actual cloudy skies, irradiance values are typically distributed between full and zero due to varying transmissivity. Shading patterns with different irradiance levels can not only reduce a PV array output but also cause multiple LMPPs and potential trapping of conventional MPPT controllers. To examine this scenario, simulations with gradual variation in irradiance levels were performed as illustrated in Fig. 15(a). Whereas SP and TCT exhibit local minima in all cases, and SP shows incipient minima in scenarios 2 and 3, all proposed S-M-TCT arrangements are found to successfully accommodate these shading pattern by allowing a more uniform distribution of shading pattern. GMPPs for all presented PV array configurations are

11[A]	32[B]	23[C]	22[G]	13[H]	31[I]	33[D]	21[E]	12[F]
21[D]	12[E]	33[F]	32[A]	23[B]	11[C]	13[G]	31[H]	22[I]
31[G]	22[H]	13[I]	12[D]	33[E]	21[F]	23[A]	11[B]	32[C]
33[C]	21[A]	12[B]	11[I]	32[G]	23[H]	22[F]	13[D]	31[E]
13[F]	31[D]	22[E]	21[C]	12[A]	33[B]	32[I]	23[G]	11[H]
23[I]	11[G]	32[H]	31[F]	22[D]	13[E]	12[C]	33[A]	21[B]
22[B]	13[C]	31[A]	33[H]	21[I]	12[G]	11[E]	32[F]	23[D]
32[E]	23[F]	11[D]	13[B]	31 [C]	22[A]	21[H]	12[I]	33[G]
12[H]	33[I]	21[G]	23[E]	11[F]	32[D]	31[B]	22[C]	13[A]

(a)

11[A]	32[A]	23[A]	11[H]	32[H]	23[H]	32[F]	23[F]	11[F]
21[A]	12[A]	33[A]	21[H]	12[H]	33[H]	12[F]	33[F]	21[F]
31[A]	22[A]	13[A]	31[H]	22[H]	13[H]	22[F]	13[F]	31[F]
23[D]	11[D]	32[D]	32[B]	23[B]	11[B]	23[I]	11[I]	32[I]
33[D]	21[D]	12[D]	12[B]	33[B]	21[B]	33[I]	21[I]	12[I]
13[D]	31[D]	22[D]	22[B]	13[B]	31[B]	13[I]	31[I]	22[I]
32[G]	23[G]	11[G]	23[E]	11[E]	32[E]	11[C]	32[C]	23[C]
12[G]	33[G]	21[G]	33[E]	21[E]	12[E]	21[C]	12[C]	33[C]
22[G]	13[G]	31[G]	13[E]	31[E]	22[E]	31[C]	22[C]	13[C]

(b)

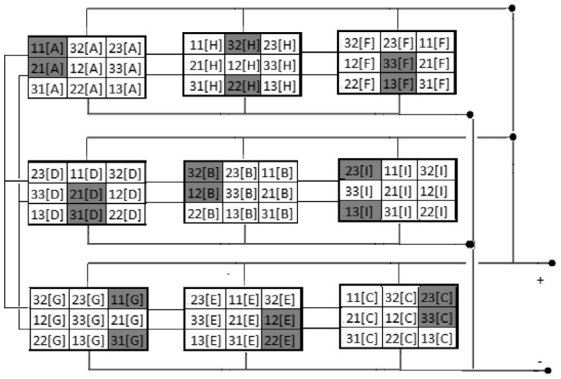

(c)

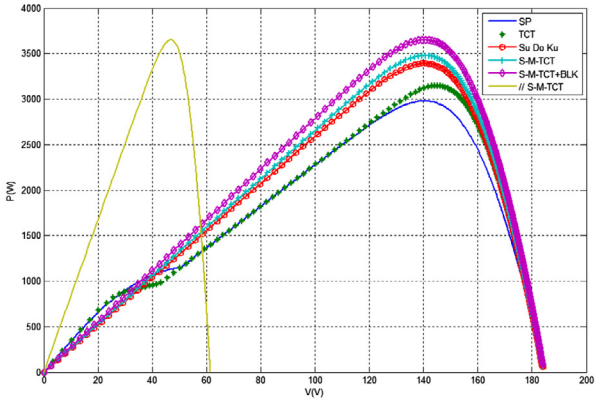

(d)

Fig. 12. Narrow and Long shading pattern: (a) S-M-TCT physical arrangement; (b) S-M-TCT electrical connection; (c) // S-M-TCT electrical connection; (d) P-V characteristics of different PV configuration.

11[A]	32[B]	23[C]	22[G]	13[H]	31[I]	33[D]	21[E]	12[F]
21[D]	12[E]	33[F]	32[A]	23[B]	11[C]	13[G]	31[H]	22[I]
31[G]	22[H]	13[I]	12[D]	33[E]	21[F]	23[A]	11[B]	32[C]
33[C]	21[A]	12[B]	11[I]	32[G]	23[H]	22[F]	13[D]	31[E]
13[F]	31[D]	22[E]	21[C]	12[A]	33[B]	32[I]	23[G]	11[H]
23[I]	11[G]	32[H]	31[F]	22[D]	13[E]	12[C]	33[A]	21[B]
22[B]	13[C]	31[A]	33[H]	21[I]	12[G]	11[E]	32[F]	23[D]
32[E]	23[F]	11[D]	13[B]	31 [C]	22[A]	21[H]	12[I]	33[G]
12[H]	33[I]	21[G]	23[E]	11[F]	32[D]	31[B]	22[C]	13[A]

(a)

11[A]	32[A]	23[A]	11[H]	32[H]	23[H]	32[F]	23[F]	11[F]
21[A]	12[A]	33[A]	21[H]	12[H]	33[H]	12[F]	33[F]	21[F]
31[A]	22[A]	13[A]	31[H]	22[H]	13[H]	22[F]	13[F]	31[F]
23[D]	11[D]	32[D]	32[B]	23[B]	11[B]	23[I]	11[I]	32[I]
33[D]	21[D]	12[D]	12[B]	33[B]	21[B]	33[I]	21[I]	12[I]
13[D]	31[D]	22[D]	22[B]	13[B]	31[B]	13[I]	31[I]	22[I]
32[G]	23[G]	11[G]	23[E]	11[E]	32[E]	11[C]	32[C]	23[C]
12[G]	33[G]	21[G]	33[E]	21[E]	12[E]	21[C]	12[C]	33[C]
22[G]	13[G]	31[G]	13[E]	31[E]	22[E]	31[C]	22[C]	13[C]

(b)

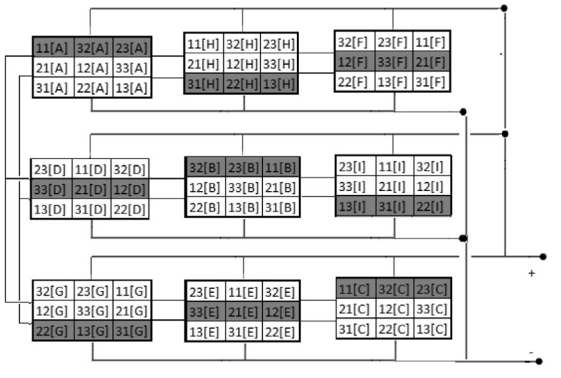

(c)

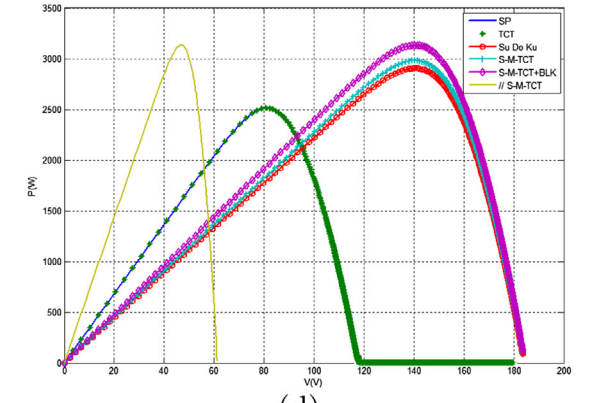

(d)

Fig. 13. Short and Wide shading pattern: (a) S-M-TCT physical arrangement; (b) S-M-TCT electrical connection; (c) // S-M-TCT electrical connection; (d) P-V characteristics of different PV configuration.

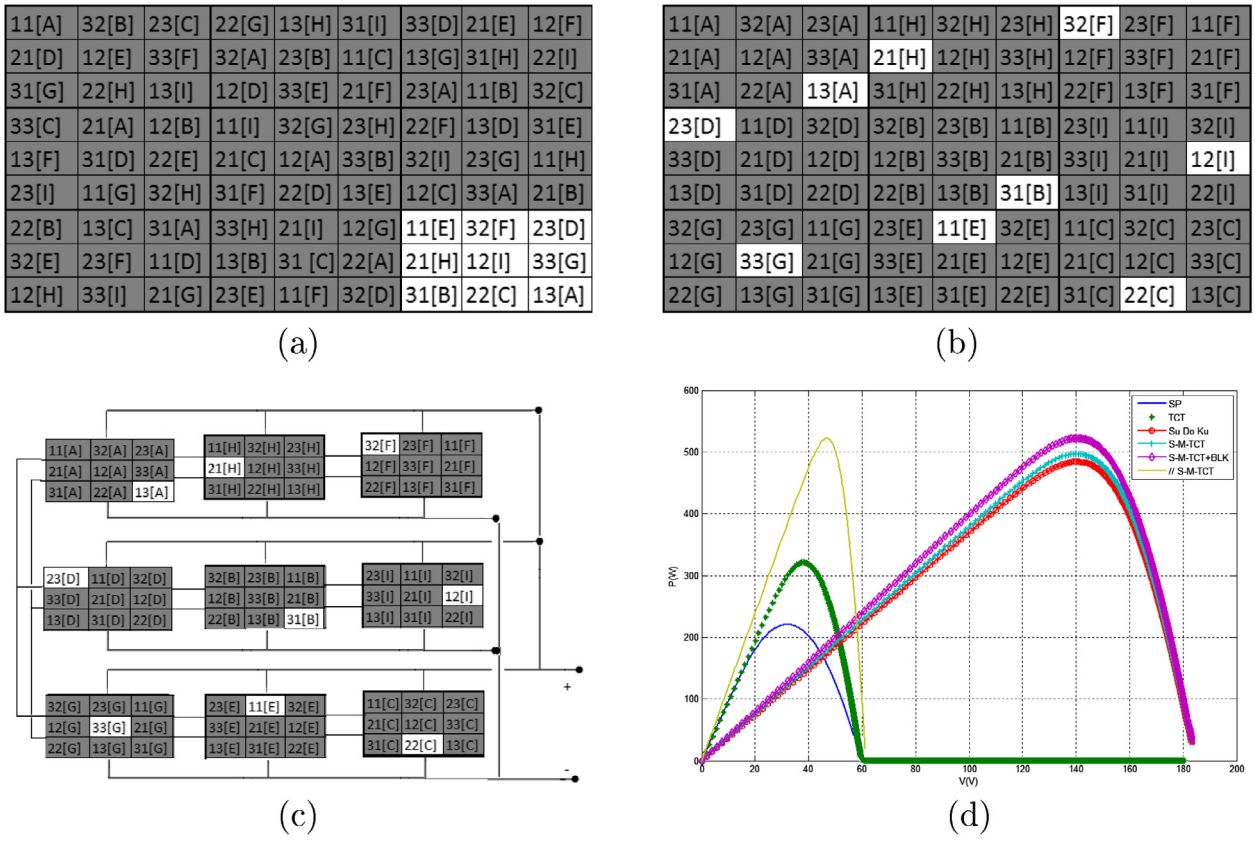

Fig. 14. Wide and Long shading pattern: (a) S-M-TCT physical arrangement; (b) S-M-TCT electrical connection; (c) S-M-TCT electrical connection; (d) P-V characteristics of different PV configuration.

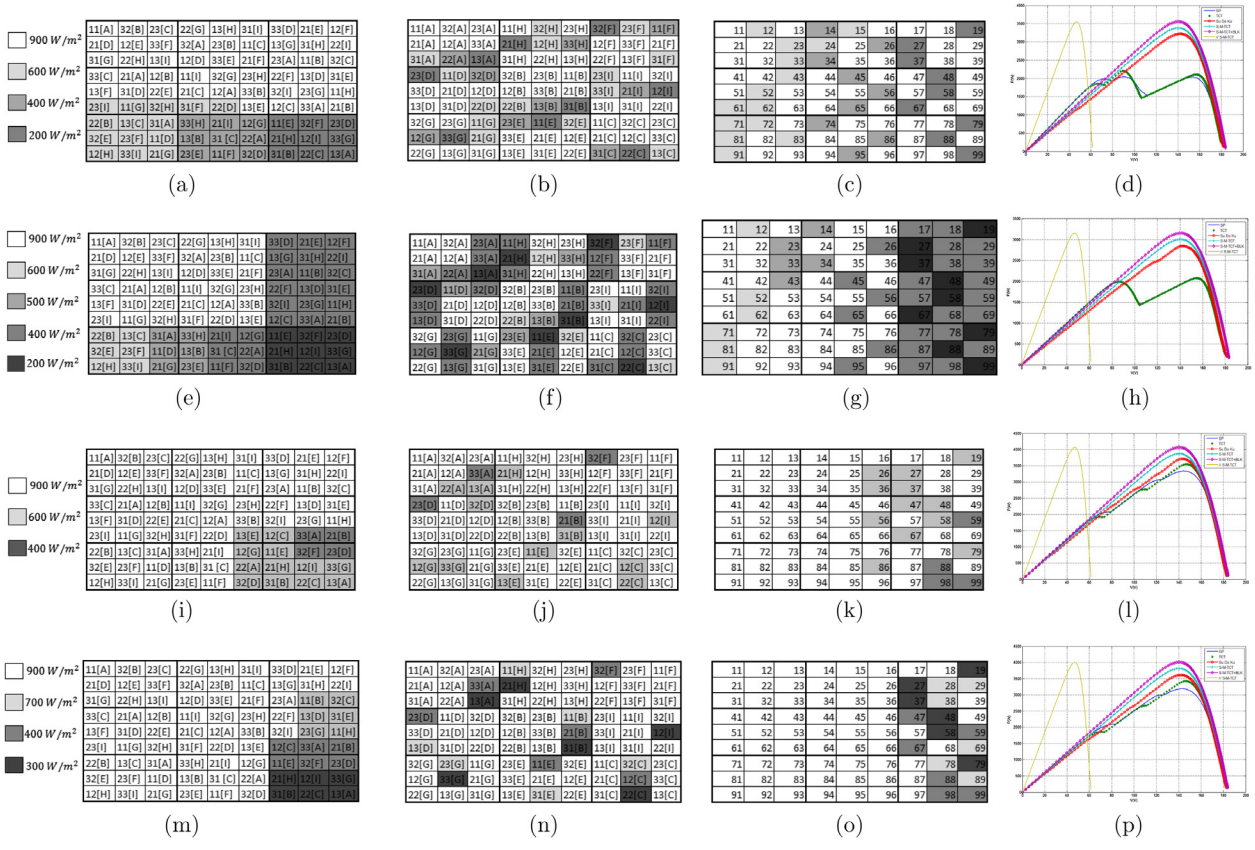

Fig. 15. Shading pattern scenarios 1–4 with different irradiation levels: S-M-TCT physical arrangement; shading dispersion using S-M-TCT arrangement; shading dispersion using Su Do Ku arrangement; P-V characteristics curves for SP, TCT, Su Do Ku, S-M-TCT, // S-M-TCT+BLK, S-M-TCT.

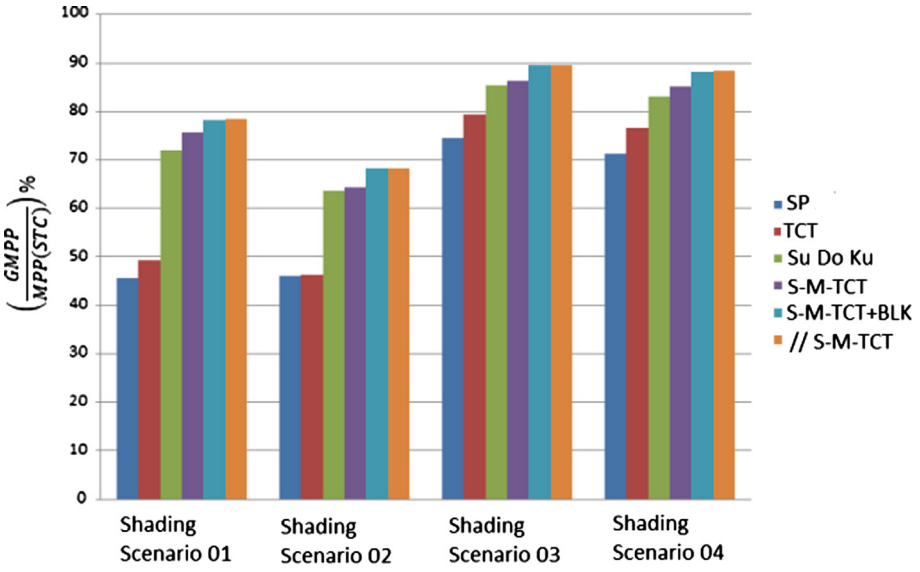

Fig. 16. GMPP (%) for the various configurations and arrangements under shading scenarios 1–4 with different irradiation levels.

summarized in Fig. 16 and show that the two S-M-TCT arrangement still generate the highest power output.

4.2.2. Partial shading pattern scenarios among the PV Sub Arrays

Three additional scenarios were considered to help examine the effect of moving clouds on the PV arrays. The scenarios considered include shaded PV modules positioned along the diagonal, across two sub arrays, and at the center of the PV array across three sub arrays, see Supplementary Material Fig. S2 for details. Under all three scenarios S-M-TCT yield equally distributed shading pattern in each row and column of the PV array. Su Do Ku distributes shading unevenly, i.e. the number of shaded PV modules in each row are not equal for the whole PV array. This results in LMPPs and a significant drop in the GMPP. Under all scenarios investigated, the S-M-TCT arrangements show enhanced PV array power output, no LMPP, and the highest GMPP.

5. Further discussion

The analysis and systematic performance assessment show that the new PV array arrangements (S-M-TCT, //S-M-TCT and S-M-TCT +BLK) are effective in reducing the impact of the partial shading. A particularly significant result is that the proposed technique outperforms previous ones *under all scenarios*: the multi-peaks problem is eliminated by the proposed PV array arrangements and effective operation is possible with no need for complicated and costly MPPT controller based on complex algorithms. In terms of PV array power output, //S-M-TCT and S-M-TCT+BLK attain almost the same GMPP (with a small difference of 1% due to the blocking diodes power dissipation), and both arrangements outperform S-M-TCT PV.

The // S-M-TCT modifies the initial S-M-TCT PV array size. Because all S-M-TCT sub arrays are connected in parallel, the new PV array columns number increases and the number of rows decreases. This reduces voltage and raises current. Furthermore, if the PV system with S-M-TCT PV array arrangement is required to feed a load (e.g. battery or grid connected appliance) with specific requirements for power, voltage and current, the parameters should be matched. The cost of the power converter to adapt the load to the PV array output should also be taken in consideration. Power conversion is not considered in either S-M-TCT and S-M-TCT +BLK PV array arrangements. The S-M-TCT+BLK PV array arrangement is based on the same S-M-TCT PV array arrangement with the addition of only blocking diodes in the top of each PV module. The blocking diodes improve appreciably the S-M-TCT PV array energy yield and minimize the partial shading effect, and their additional cost to the system is minimal since they are inexpensive. We finally note that the proposed PV array arrangements are all connected with a TCT configuration; they generally have the same interconnections and total and they will therefore have the same total wire resistance.

6. Conclusions

This paper proposes three new physical PV array arrangements (S-M-TCT, S-M-TCT+BLK and // S-M-TCT) that can be used in PV arrays of any size to mitigate partial shading effects. The proposed arrangements were systematically analyzed under a range of shading scenarios and compared to several existing techniques/arrangements, and were shown to enhance PV power output, minimizes protection diode power dissipation and eliminate the multiple peaks (LMPPs) in the P-V characteristics under severe partial shading conditions. These PV arrangements distribute the shading pattern uniformly over the entire array and generate a single MPP that corresponds to the GMPP, thus allowing easy tracking of the MPP with a simple MPPT controller, dispensing with complex algorithms and costly hardware.

All three variants of the S-M-TCT arrangement enhance GMPP for all types of shading pattern considered when compared to other existing arrangements and configurations. // S-M-TCT and S-M-TCT +BLK perform very closely and yield higher power output under all shading scenarios considered. Specifically, compared to the reference SP arrangement, the performance gains range from about 19% under elongated cloud patterns to over 140% for larger (wide-long) cloud patterns. The Su Do Ku arrangement also achieves some (smaller) gains ranging from 2 to 14%, and generally exhibits a single peak, but it encounters problems under shading scenarios mimicking moving clouds, for which it distributes shading unevenly and produces local maxima (LMPPs).

The new shift modified TCT arrangements are suitable for both grid connected and off-grid applications, and though the analysis and performance of these arrangements was presented for up to 9×9 PV arrays, the concept is not limited to these array sizes. The extension of the proposed concept to any arbitrary PV array

size in conjunction with the development of a generalized algorithm will be the focus of future work.

Acknowledgements

Funding and technical support for this work was provided by the Deanship of Scientific Research, King Abdulaziz University, Jeddah, under Grant No. (1-135-36-HiCi), and by the Natural Sciences and Engineering Research Council of Canada. NB's stay at the University of Victoria was also funded in part by a PNE Grant from the Algerian Ministry of Higher Education and Scientific Research.

Appendix A. Supplementary material

Supplementary data associated with this article can be found, in the online version, at http://dx.doi.org/10.1016/j.apenergy.2016.11.038.

References

[1] Kuang Y, Zhang Y, Zhou B, Li C, Cao Y, Li L, et al. A review of renewable energy utilization in islands. Renew Sustain Energy Rev 2016;59:504–13.
[2] Cancino-Solórzano Y, Paredes-Sánchez JP, Gutiérrez-Trashorras AJ, Xiberta-Bernat J. The development of renewable energy resources in the state of Veracruz, Mexico. Utilit Policy 2016;39:1–4.
[3] Sahoo SK. Renewable and sustainable energy reviews solar photovoltaic energy progress in India: a review. Renew Sustain Energy Rev 2016;59:927–39.
[4] Pareek S, Dahiya R. Enhanced power generation of partial shaded photovoltaic fields by forecasting the interconnection of modules. Energy 2016;95:561–72.
[5] Murtaza A, Chiaberge M, Spertino F, Boero D, De Giuseppe M. A maximum power point tracking technique based on bypass diode mechanism for PV arrays under partial shading. Energy Build 2014;73:13–25.
[6] Rizzo SA, Scelba G. ANN based MPPT method for rapidly variable shading conditions. Appl Energy 2015;145:124–32.
[7] Ahmed J, Salam Z. A critical evaluation on maximum power point tracking methods for partial shading in PV systems. Renew Sustain Energy Rev 2015;47:933–53.
[8] Ishaque K, Salam Z. A review of maximum power point tracking techniques of PV system for uniform insolation and partial shading condition. Renew Sustain Energy Rev 2013;19:475–88.
[9] Eltawil MA, Zhao Z. MPPT techniques for photovoltaic applications. Renew Sustain Energy Rev 2013;25:793–813.
[10] Alajmi BN, Ahmed KH, Finney SJ, Williams BW. A maximum power point tracking technique for partially shaded photovoltaic systems in microgrids. IEEE Trans Ind Electron 2013;60(4):1596–606.
[11] Liu YH, Liu CL, Huang JW, Chen JH. Neural-network-based maximum power point tracking methods for photovoltaic systems operating under fast changing environments. Sol Energy 2013;89:42–53.
[12] Daraban S, Petreus D, Morel C. A novel MPPT (maximum power point tracking) algorithm based on a modified genetic algorithm specialized on tracking the global maximum power point in photovoltaic systems affected by partial shading. Energy 2014;74:374–88.
[13] Salam Z, Ahmed J, Merugu BS. The application of soft computing methods for MPPT of PV system: a technological and status review. Appl Energy 2013;107:135–48.
[14] Deshkar SN, Dhale SB, Mukherjee JS, Babu TS, Rajasekar N. Solar PV array reconfiguration under partial shading conditions for maximum power extraction using genetic algorithm. Renew Sustain Energy Rev 2015;43:102–10.
[15] Srinivasa Rao P, Saravana Ilango G, Nagamani C. Maximum power from PV arrays using a fixed configuration under different shading conditions. IEEE J Photovolt 2014;4(2):679–86. doi: http://dx.doi.org/10.1109/JPHOTOV.2014.2300239.
[16] Villa LFL, Picault D, Raison B, Bacha S, Labonne A. Maximizing the power output of partially shaded photovoltaic plants through optimization of the interconnections among its modules. IEEE J Photovolt 2012;2(2):154–63.
[17] Malathy S, Ramaprabha R. Comprehensive analysis on the role of array size and configuration on energy yield of photovoltaic systems under shaded conditions. Renew Sustain Energy Rev 2015;49:672–9.
[18] La Manna D, Vigni VL, Sanseverino ER, Di Dio V, Romano P. Reconfigurable electrical interconnection strategies for photovoltaic arrays: a review. Renew Sustain Energy Rev 2014;33:412–26.
[19] Karatepe E, Boztepe M, Colak M. Development of a suitable model for characterizing photovoltaic arrays with shaded solar cells. Sol Energy 2007;81(8):977–92.
[20] Kadri R, Andrei H, Gaubert JP, Ivanovici T, Champenois G, Andrei P. Modeling of the photovoltaic cell circuit parameters for optimum connection model and real-time emulator with partial shadow conditions. Energy 2012;42(1):57–67.
[21] Velasco-Quesada G, Guinjoan-Gispert F, Pique-Lopez R, Roman-Lumbreras M, Conesa-Roca A. Electrical PV array reconfiguration strategy for energy extraction improvement in grid-connected PV systems. IEEE Trans Ind Electron 2009;56(11):4319–31.
[22] Tian H, Mancilla-David F, Ellis K, Muljadi E, Jenkins P. Determination of the optimal configuration for a photovoltaic array depending on the shading condition. Sol Energy 2013;95:1–12.
[23] Parlak KŞ. PV array reconfiguration method under partial shading conditions. Int J Electr Power Energy Syst 2014;63:713–21.
[24] Villa LFL, Ho TP, Crebier JC, Raison B. A power electronics equalizer application for partially shaded photovoltaic modules. IEEE Trans Ind Electron 2013;60(3):1179–90.
[25] Potnuru SR, Pattabiraman D, Ganesan SI, Chilakapati N. Positioning of PV panels for reduction in line losses and mismatch losses in PV array. Renew Energy 2015;78:264–75.
[26] Rani BI, Ilango GS, Nagamani C. Enhanced power generation from PV array under partial shading conditions by shade dispersion using Su Do Ku configuration. IEEE Trans Sustain Energy 2013;4(3):594–601.
[27] Sahu HS, Nayak SK. Power enhancement of partially shaded PV array by using a novel approach for shade dispersion. In: Innovative smart grid technologies-Asia (ISGT Asia), 2014 IEEE. IEEE; 2014. p. 498–503.
[28] Celik B, Karatepe E, Silvestre S, Gokmen N, Chouder A. Analysis of spatial fixed PV arrays configurations to maximize energy harvesting in BIPV applications. Renew Energy 2015;75:534–40.
[29] Vijayalekshmy S, Bindu G, Iyer SR. A novel zig-zag scheme for power enhancement of partially shaded solar arrays. Sol Energy 2016;135:92–102.
[30] Yadav AS, Pachauri RK, Chauhan YK. Comprehensive investigation of PV arrays with puzzle shade dispersion for improved performance. Sol Energy 2016;129:256–85.
[31] Jena D, Ramana VV. Modeling of photovoltaic system for uniform and non-uniform irradiance: a critical review. Renew Sustain Energy Rev 2015;52:400–17.
[32] Dizqah AM, Maheri A, Busawon K. An accurate method for the PV model identification based on a genetic algorithm and the interior-point method. Renew Energy 2014;72:212–22.
[33] Brano VL, Ciulla G. An efficient analytical approach for obtaining a five parameters model of photovoltaic modules using only reference data. Appl Energy 2013;111:894–903.
[34] Ishaque K, Salam Z, Taheri H. Simple, fast and accurate two-diode model for photovoltaic modules. Sol Energy Mater Sol Cells 2011;95(2):586–94.
[35] Ishaque K, Salam Z, Taheri H, et al. Modeling and simulation of photovoltaic (PV) system during partial shading based on a two-diode model. Simul Model Pract Theory 2011;19(7):1613–26.
[36] Ishaque K, Salam Z, et al. A comprehensive MATLAB Simulink PV system simulator with partial shading capability based on two-diode model. Sol Energy 2011;85(9):2217–27.
[37] Belhaouas A, Cheikh A, Larbes C. Suitable Matlab-Simulink simulator for PV system based on a two-diode model under shading conditions. In: 2013 3rd international conference on systems and control (ICSC). IEEE; 2013. p. 72–6.
[38] Bastidas-Rodriguez JD, Ramos-Paja CA, Saavedra-Montes AJ. Reconfiguration analysis of photovoltaic arrays based on parameters estimation. Simul Model Pract Theory 2013;35:50–68.
[39] Chao KH, Lin YS, Lai UD. Improved particle swarm optimization for maximum power point tracking in photovoltaic module arrays. Appl Energy 2015;158:609–18.
[40] Reinoso CRS, Milone DH, Buitrago RH. Simulation of photovoltaic centrals with dynamic shading. Appl Energy 2013;103:278–89.
[41] El-Dein MS, Kazerani M, Salama M. An optimal total cross tied interconnection for reducing mismatch losses in photovoltaic arrays. IEEE Trans Sustain Energy 2013;4(1):99–107.
[42] Silvestre S, Boronat A, Chouder A. Study of bypass diodes configuration on PV modules. Appl Energy 2009;86(9):1632–40.
[43] Kato K, Koizumi H. A study on effect of blocking and bypass diodes on partial shaded PV string with compensating circuit using voltage equalizer. In: 2015 IEEE international symposium on circuits and systems (ISCAS). p. 241–4. doi: http://dx.doi.org/10.1109/ISCAS.2015.7168615.
[44] Kim K, Krein P. Reexamination of photovoltaic hot spotting to show inadequacy of the bypass diode. IEEE J Photovolt 2015;5(5):1435–41. doi: http://dx.doi.org/10.1109/JPHOTOV.2015.2444091.
[45] Zheng H, Li S, Challoo R, Proano J. Shading and bypass diode impacts to energy extraction of PV arrays under different converter configurations. Renew Energy 2014;68:58–66.